Imaging and Radiation Research (2022) Volume 5 Issue 1
doi:10.24294/irr.v5i1.1748

REVIEW ARTICLE

3D ultrasound in cardiology

Antonio J Bravo[1]*, Miguel Vera[2,3], Delia Madriz[4], Julio Contreras-Velásquez[3], José Chacón[2], Sandra Wilches-Durán[2], Modesto Graterol-Rivas[2], Daniela Riaño-Wilches[6], Joselyn Rojas[5], Valmore Bermúdez[7]

[1] Coordinación de Investigación Industrial, Decanato de Investigación, Universidad Nacional Experimental del Táchira, Táchira, Venezuela. E-mail: abravo@unet.edu.ve*

[2] Grupo de Investigación Altos Estudios de Frontera (ALEF), Universidad Simón Bolívar, Cúcuta, Colombia.

[3] Grupo de Investigación en Procesamiento Computacional de Datos (GIPCD-ULA) Universidad de Los Andes-Táchira, Venezuela.

[4] Programa Calidad y Productividad Organizacional, Decanato de Investigación, Universidad Nacional Experimental del Táchira, Táchira, Venezuela.

[5] Pulmonary and Critical Care Medicine Department, Brigham and Women's Hospital, Harvard Medical School, Boston, USA.

[6] Facultad de Medicina, Universidad de los Andes, Bogotá, Colombia.

[7] Centro de Investigaciones Endocrino-Metabólicas "Dr. Félix Gómez" Facultad de Medicina, Universidad del Zulia, Venezuela.

ABSTRACT

Cardiovascular imaging analysis is a useful tool for the diagnosis, treatment and monitoring of cardiovascular diseases. Imaging techniques allow non-invasive quantitative assessment of cardiac function, providing morphological, functional and dynamic information. Recent technological advances in ultrasound have made it possible to improve the quality of patient treatment, thanks to the use of modern image processing and analysis techniques. However, the acquisition of these dynamic three-dimensional (3D) images leads to the production of large volumes of data to process, from which cardiac structures must be extracted and analyzed during the cardiac cycle. Extraction, three-dimensional visualization, and qualification tools are currently used within the clinical routine, but unfortunately require significant interaction with the physician. These elements justify the development of new efficient and robust algorithms for structure extraction and cardiac motion estimation from three-dimensional images. As a result, making available to clinicians new means to accurately assess cardiac anatomy and function from three-dimensional images represents a definite advance in the investigation of a complete description of the heart from a single examination. The aim of this article is to show what advances have been made in 3D cardiac imaging by ultrasound and additionally to observe which areas have been studied under this imaging modality.

Keywords: Ultrasound; Acquisition; Visualization; Processing; Reconstruction; Cardiology

ARTICLE INFO

Received: 20 February 2022
Accepted: 1 April 2022
Available online: 6 April 2022

1. Introduction

In the last three decades, the construction and visualization of three-dimensional images from ultrasound data has been a topic of interest for a large group of researchers inspired, basically, by the fact that 3D ultrasound (US) allows visualization of image planes that are not accessible in 2D ultrasound[1].

Ultrasound images are essentially a measure of the acoustic response of an impulse at a particular frequency. For high frequencies around 15 MHz, very good resolution is obtained, but the scan is only a few centimeters deep, while for

low frequencies around 3 MHz, they generate images of very poor resolution, allowing the scanning of tissues at depths of 25 cm or more. Each ultrasound image is composed of a set of fringes acquired sequentially in time and space. Each fringe represents the amplitude of the response of an ultrasound pulse at the location and in the direction, it is generated (constant velocity sound is assumed to relate this response to the depth within the patient). Since the magnitude decays exponentially with depth, a logarithmic operator with an associated weight factor must be applied to the fringe before it is quantified and represented as a grayscale image. The image thus generated corresponds to a B-scan, which is one of several different images produced using ultra-sound. The types depend on how the response to the acoustic impulse is displayed, hence there are "A", "B", "C" and "M" modes. **Figure 1** schematizes the process of generating an ultrasound image, a more detailed description of the process can be found in Kremkau[2].

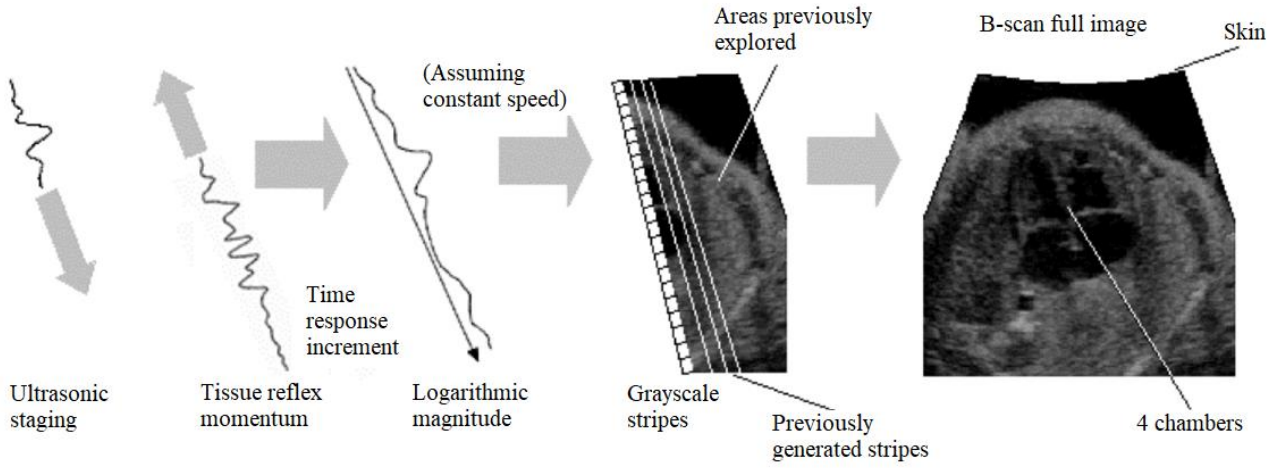

Figure 1. Ultrasound image generation.

The 2D ultrasound imaging process assumes that the ultrasound pulses sweep the tissue along a straight line and that the speed of sound is constant, which is not entirely true, because the interaction of ultrasound with living tissue generates anisotropic and nonlinear effects such as absorption, diffraction, refraction and reflection, further altering the propagation velocity of the acoustic wave[2]. Parameters such as tissue attenuation, frequency, pulse length, resolution, bandwidth, pulse amplitude, transmitted pulse shape and repetition frequency are all interrelated in the ultrasound imaging process.

Various sources of noise, including thermal noise of the amplification circuits, acoustic noise, phase effects (noise speckle), as well as the type, size and texture of the transducer, constitute elements of distortion that generate artifacts in ultrasound images[3]. However, image quality, thanks to technological evolution, is continuously improving[4-9]. The greatest advantage of 2D ultrasound is its flexibility, which allows the specialist to manipulate the transducer and visualize the desired anatomical section.

With the use of conventional 2D ultrasound, only a very thin section of the patient can be imaged at the same time, and the location of that image plane is controlled by the manual orientation of the transducer. This implies that the operator must perform a mental integration of some 2D images in order to generate the 3D anatomy or pathology, which makes this imaging process slow, non-reproducible over time; and most importantly, subject to the operator's experience[10].

The objective of 3D ultrasound imaging is to overcome these limitations by providing techniques that reduce the variability introduced by conventional techniques, and to allow the specialist to visualize the anatomy in 3D. The increasing importance of ultrasound in clinical diagnosis, coupled with optimal transducer design, rapid improvements in computer performance and cost ratio, is rapidly pushing conventional clinical imaging toward 3D imaging. As a result, the great potential of 3D ultrasound in clinical diagnostic and therapeutic ap-

plications has been exploited[11-16], and 3D ultrasound imaging systems are now routinely used in clinical studies[17].

This article describes the clinical utility and technological advances of 3D ultrasound imaging, particularly oriented to the understanding and visualization of the structures of the heart and their variations throughout the cardiac cycle. The main acquisition techniques used are presented, followed by a review of the various methods used in 3D reconstruction and visualization processes, and finally some of the advances obtained in three-dimensional echocardiography (3DE) are shown.

2. Three-dimensional acquisition techniques

In a 3D ultrasound system, the location of the acoustic signal is known in three dimensions. This allows a complete representation of the volume of the structure or tissue to be imaged. In general, ultrasound is a real-time imaging modality, and 3D ultrasound also has the great possibility of displaying information at speeds very close to real time, which is basically due to the delay introduced by the processing systems. High acquisition rates of the order of 10–60 images per second can be provided by some 3D ultrasound systems[18].

Most 3D ultrasound systems use a conventional ultrasound transducer to acquire a series of 2D images and differ only in the method used to determine the position and orientation of those 2D images with respect to the volume under examination. These transducers are composed of a 1D (N × 1) linear array of more than 100 electronic elements that steer and focus the ultrasound beam. For this type of system, two acquisition methods have been reported: freehand and fixed geometry.

Other 3D ultrasound systems use transducers composed of 2D arrays, which allow acquisition of multiple planes of a given volume in real time. In addition, it is possible to scan for vascular pathologies with the help of acquisition systems that use intravascular ultrasound.

2.1 Freehand acquisition

The images are acquired with arbitrary position and direction controlled by the operator. In freehand scanning, the movement of the transducer is controlled by the operator in the same way as in conventional ultrasound. The position and orientation of the transducer are determined by a position sensor attached to the transducer. The special advantage of this technique over fixed geometry is that the operator can select optimal views and orientations, adjusting the transducer to the complex surface of the patient. Several technologies have been developed for position determination: magnetism, sound, light and electricity.

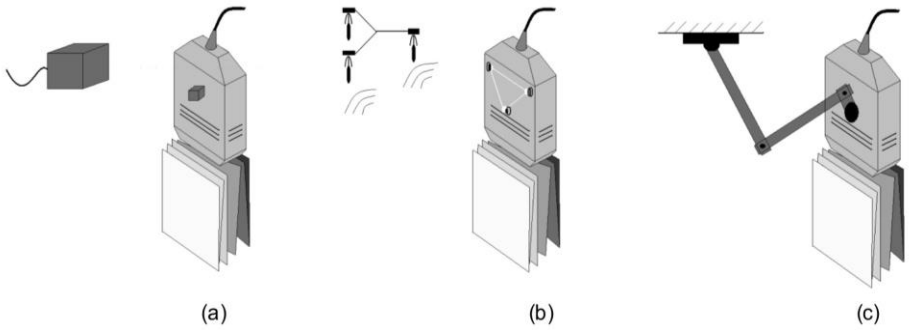

Figure 2. Schematic diagrams showing the three basic methods for obtaining the position and orientation of ultrasound transducers for the freehand acquisition technique. Note: **(a)** Magnetics in ultrasound; **(b)** acoustics; **(c)** electricity.

2.1.1 Magnetic

The principle of operation of these devices is the reduction of the energy of the magnetic field generated by the electric current sent through three small orthogonal wires, which constitute a remote transmitter, arranged in a cubic structure placed very close to the patient[19]. The receiver is placed over the transducer and is composed of a set of wires of approximately 2.5 cm in each dimension. **Figure 2(a)** shows the schematic of a positioning system based on the magnetic method. By measuring the magnetic field, the angle and position of the

receiver relative to the transmitter can be determined. There are two types of sensors; one using alternating current (AC), and one using direct current (DC). Each of these sensors is affected by the presence of certain materials (metals, surgical, ultrasound probes) near them; metallic materials affect AC sensors, while ferromagnetic materials affect DC sensors[20].

2.1.2 Acoustics

The acoustic method works by attaching a wave emitter in an acoustic range to the transducer and collecting those signals by three remote microphones, which positioned in different orientations (not necessarily orthogonal), and typically placed over the patient. A schematic of this positioning technology can be seen in **Figure 2(b)**. The operator freely moves the transducer over the patient while the sound emitting device is activated. Knowing the speed of sound in the air, the position of the microphones and the time of flight of the sound pulses, the angle and position of the transducer can be continuously monitored[21]. One of the limitations of this positioning method is that the microphones must be placed close to the patient, so that there is no obstruction of the lines of sight of the transmitter to the receiver, and they must be close enough to the transducer to be able to detect the sound pulses.

2.1.3 Optics

The optical method works in a similar way to the acoustic method, except that the emitter is replaced by at least three infrared LEDs. An infrared light emitting diode (LED) is an opto-electronic component capable of emitting light outside the visible spectrum when an electric current is circulated. The main problem with the optical method is that the lines of sight between the LEDs and the optical sensor can never be lost[22].

2.1.4 Electrical

Several systems have used mechanical arms with different degrees of freedom[18,23]. The transducer is mounted on a mechanical arm system with multiple movable joints, as shown in **Figure 2©**, which allows the operator to manipulate the transducer in a complex manner to select the desired view and orientation. A set of potentiometers are placed at the joints of the mechanical arm, and any movement at the joints is re-recorded and stored. From the records, the angle and position of the transducer can be continuously calculated and monitored.

2.2 Acquisition by fixed geometry

In fixed geometry scanning, the transducer movement is partially or completely controlled by a mechanical system based on stepper motors; in this sense, the position and orientation of the transducer are preset. Mechanical systems produce very regular data sets, which simplifies post-processing and ensures uniform coverage of the scanned volume. On the other hand, this type of system allows scanning volumes as large as the volume itself admits. The coordinates of the reference frame are set according to the housing mechanism of the stepper motor; the larger the stepper motor, the larger the scanning area. Very large systems are difficult to manipulate in practice, since the transducer must maintain good contact with the skin surface at all times.

Excessive pressure from transducer contact with the skin can cause the anatomic baseline to move, resulting in erroneous data being recorded. Ultrasound systems incorporating this type of acquisition technique use a motorized drive mechanism that moves or rotates the transducer while 2D ultrasound images are acquired at predefined spatial intervals. The predefined geometry for the two-dimensional image acquisition process allows for fast and accurate 3D image reconstruction immediately after the scan. As the 3D image is produced from a series of conventional 2D ultrasound images, its resolution will not be isotropic. In the direction parallel to the planes of the acquired 2D images, the resolution is the same as that of the 2D images, but in the direction of the 3D scan, it will depend on the spatial sampling rate, which in this type of system defines the maximum resolution of the transducer. Therefore, the resolution of the 3D image will generally be lower in the scan direction. Typically, 200 images are acquired at 0.5 mm intervals for 3D B-scan. This technology has been implemented in basically three types of motion: linear, sector and

rotation, as shown in **Figure 3**.

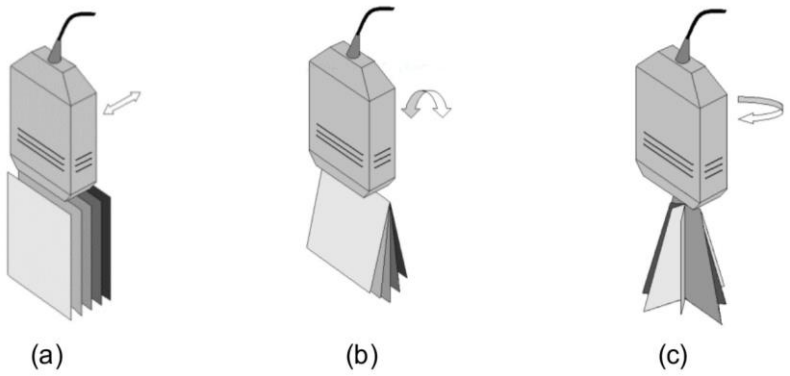

Figure 3. Schematic diagrams of the three basic types of motion used in 3D ultrasound systems with fixed geometry acquisition technology. Note: **(a)** linear; **(b)** sector; **(c)** rotation.

2.2.1 Linear

The transducer is mechanically translated in a linear fashion, parallel to the patient's skin and perpendicular to the imaging plane. The acquired 2D images are parallel to each other and separated by predefined intervals, as shown in **Figure 3(a)**, which establishes a minimal degradation of the 3D information, allowing a considerably efficient reconstruction process.

2.2.2 Sector

Figure 3(b) shows a transducer that is rotated about its axial direction, thus allowing an angular sweep to be performed, generating a range of planes that are acquired with a preset angular separation and that define the scanned volume. The advantage of this technique is that the mechanisms that integrate it can be produced sufficiently small, so that it is easy to manipulate.

2.2.3 Rotation

In this scanning geometry, the transducer is placed on a mechanical system that rotates it on its central axis (see **Figure 3(c)**). In this way, the acquired images are positioned over the patient according to a helix-shaped cone. The acquired planes intersect in the center of the cone along the axis of rotation, so no movement is allowed at the time of the scan because this would cause an inconsistency in the acquired planes, generating the distortion of the resulting image in its center, along the axis of rotation.

2.3 Acquisition by two-dimensional arrays

In the previous two sections, it has been shown that a 3D volume can be constructed by translation, rotation and by rocking the ultrasound transducer with the aid of a mechanical device, such that the spatial relationship between the acquired 2D images is known. Alternatively, the 3D volume can be created by freehand manipulation of the transducer, whose orientation is continuously stored by means of a wireless 3D locator. Regardless of the transducer localization mechanism, such solutions are slow compared to the dynamics of some organs such as the heart. Systems assisted by electro-cardiogram and respiratory signals have been designed for the reconstruction of 3D images of the heart in multiple cardiac cycles, but such data still present distortions, generated by cardiac arrhythmias and irregular breathing.

Real-time ultrasound imaging is one of the most recent advances in ultrasound imaging. In this type of technology, it is necessary to use transducers composed of 2D arrays (N × M), which allow the ultrasound beam to be dynamically directed and focused as a pyramid (see **Figure 4**), producing a volume of data[24]. The information in the three dimensions is localized by the physical movement of the transducer, either using mechanical means or by manual operation.

The echoes that generate the pyramidal shape are processed to generate 3D information in real time[25]. This represents great advantages in the acquisition of 3D ultrasound images. However, some problems must be overcome, such as the low operating ranges, approximately 2.5 MHz, due to the

large number of small elements (N × M) that must be incorporated and their difficult connectivity process[18,25].

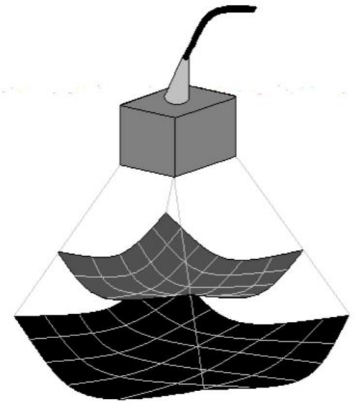

Figure 4. Schematic diagram showing a 2D array used in a 3D ultrasound system.

2.4 Intravascular acquisition

Intravascular ultrasound imaging (IVUS) is a relatively new technique that allows visualization of the internal structure of the arteries in a highly detailed way[11,26] with the help of miniature ultrasound transducers placed at the tip of a catheter, whose main characteristic is that it corresponds to the same one used in contrast coronagraph. The catheter is introduced into the patient's arterial system through an artery in the thigh, maneuvering through the descending aorta, around the aortic arch and into the coronary arteries.

Table 1. Three-dimensional ultrasound scanning methods

Exploration method		Image acquisition method
Freehand	Magnetic	Measurement of the magnetic field generated by a transmitter placed next to the patient with the receiver placed over the transducer.
	Acoustics	Measurement of the time of flight of the sound signal emitted by the transducer and picked up by microphones located near the patient.
	Optics	Measurement of infrared rays emitted by an array of LEDs located on the transducer that are sent to receivers located near the patient.
	Electric	Measurement of the angle between moving arms.
Fixed geometry	Linear	The acquired 2D images are parallel to each other and equally spaced.
	Sector	The acquired 2D images form a fan of pianos with fixed angle of separation.
	Rotational	The acquired images sweep a conical volume in the form of helices.
2D arrangements		2D arrays transmit a pyramidal beam and the returned echoes are displayed as multiple planes in real time.
Intravascular		The images are acquired by rotating a miniature transducer that is placed on the tip of a catheter, which is introduced into the arterial system.

By rotating the transducer, images of cut sections are generated by emitting ultrasound pulses (20–50 MHz) which, after a time delay, are received as echoes. The main advantage of IVUS over contrast angiography is that it can generate images of the internal structure of the artery wall. Clearly, the major advantage of 3D IVUS is that it provides detailed 3D images with high resolution over small vascular regions of interest (1–5 cm^3). **Table 1** shows a summary about 3D ultrasound scanning methods.

3. Three-dimensional reconstruction

Reconstruction refers to the process by which the acquired 2D images are placed in the correct position and orientation in the 3D volume, and with the values associated to their pixels the voxel value in the corresponding 3D image is determined. The first step is to determine the coordinate system where the 2D images are integrated into the volume image, placing each pixel in its corresponding 3D coordinate (x, y, z). This process can be implemented with spatial transformation models[27], which differ in both freehand and fixed geometry exploitation. Based on the 2D coordinates (x, y) of each pixel in its 2D image, position and orientation are obtained from the scanning method used in the freehand acquisition stage. It should be considered that in fixed geometry acquisition, the spatial location of the image pixels is known. The value of the voxels can be determined by applying an interpolation process. The weights associated with the interpolation process can be pre-calculated and placed in a lookup table, allowing the reconstruction to be considerably faster[18]. In 3D ultrasound, there are basically two reconstruction methods: fea-

ture-based reconstruction and voxel-based reconstruction.

3.1 Coordinate system in freehand 3D scanning

Figure 5 shows the four coordinate systems used for the reconstruction. *I* is the coordinate system of the 2D image. The x-axis is in the lateral direction, and the y-axis is in the axial direction. *R* is the coordinate system of the position sensor and *T* is the coordinate system of the transmitter. The volume created from the acquired 2D images takes the form of an array *V* of 3D voxels, placed on the coordinate system *V*. Each pixel (${}^{I}\mathrm{x}$) is transformed first to the coordinate system of the receiver *R*, then to the transmitter *T* and finally to the reconstructed volume *V*. The whole transformation process can be expressed as the multiplication of homogeneous transformation matrices, according to equation 1.

$$ {}^{V}\mathrm{x} = {}^{V}\mathrm{T}_{T} \cdot {}^{T}\mathrm{T}_{R} \cdot {}^{R}\mathrm{T}_{I} \cdot {}^{I}\mathrm{x} \quad (1) $$

in which,

$$ {}^{I}\mathrm{x} = \begin{bmatrix} s_x u \\ s_y v \\ 0 \\ 1 \end{bmatrix} \quad (2) $$

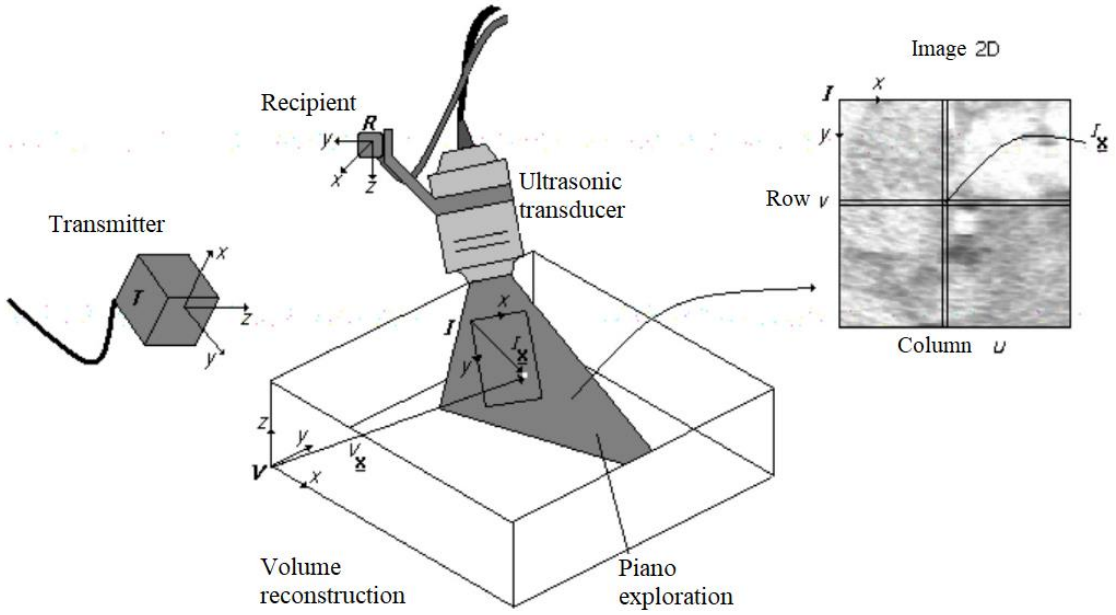

Figure 5. Coordinate systems used in 3D reconstruction.

A standard notation is adopted. ${}^{K}\mathrm{T}_{L}$ is the transformation from the coordinate system *L* to the system *K*. *u* and *v* represent the indices of the columns and filas of the 2D image, and s_x and s_y the scale factors in mm/pixel. ${}^{V}\mathrm{x}$ represents the location of the voxel in the *V* coordinate system.

A transformation between two three-dimensional coordinate systems has six degrees of freedom: three translations (x, y, z) and three rotations (a, b, g). Each of the matrices in equation 1 plays a different role in the reconstruction. ${}^{T}\mathrm{T}_{R}$ is obtained directly from the sensor reading. ${}^{V}\mathrm{T}_{T}$ is considered a convenience transformation. It can be omitted by assuming that the volume to be reconstructed is aligned with the transmitter, which could cause problems if, for example, the B-scan passes through the origin of *V*, generating a large empty voxel. This type of effect can be corrected by setting an arbitrary ${}^{V}\mathrm{T}_{T}$ transform, defined at each scan. ${}^{R}\mathrm{T}_{I}$ and the scale factors s_x and s_y are determined by calibration[28]. The voxel position ${}^{V}\mathrm{x}$ can then be calculated from equation 1 and assigned a value according to the intensities of the intersecting pixels[29-31].

3.2 Coordinate system in fixed geometry scanning

In fixed geometry scanning, the transducer is rigidly mounted on a mechanical device, which, according to a certain protocol, generally controlled by a computer, scans the object by translation, fanning and rotation of the transducer. An extensive review of the transformations of fixed geometry systems to obtain the location of the voxel

in the reconstructed space can be found in Tong[32] and Cardinal[33].

3.3 Feature-based reconstruction

In this method, a specific feature is initially determined and then reconstructed on the 3D image. In echocardiography or obstetrics, the ventricle or fetal structure can be delineated (manually or automatically) on the 2D images, and then the surface reconstruction is made from these contours. The segmentation of the structures in the 2D images is considered the most important step in this type of reconstruction because there is no efficient and stable method to accurately extract the edges of the anatomical structure. Different techniques for the detection of epicardial and endocardial borders from ultrasound images have been reported. Models based on Markov random fields[34,35], fuzzy logic[36], neural networks[6,37], morphological filters[38] and active contours[39-42] have been proposed. Similar techniques have been used in the three-dimensional reconstruction of intravascular ultrasound images[11,26].

3.4 Voxel-based reconstruction

In this type of method, the extraction of a certain feature is not necessary to perform the reconstruction. From the set of acquired 2D images, a voxel-based image (Cartesian regular grid of volume elements in three dimensions) is constructed. Then, the voxel value can be set according to the intensities of the intersecting pixels. In general, this can be treated as an optimization problem, in which given a similarity criterion or registration quality criterion, its global optimum must be found in a predefined space of geometric transformations, which corresponds to the volume image. One of the first applications based on voxel similarity for ultra-sound volume registration was proposed by Rohling[29]. Additionally, methods based on gradients[30] and others based on surface deformations[31] have been proposed.

The voxel-based method guarantees the preservation of information originally contained in the acquired 2D images. Hence, if appropriate cut sections of the 3D image are performed, the original 2D image can be recovered. On the other hand, if in the scanning process the sampling of the 3D structure is not performed properly, so that gaps occur between the 2D images, in the reconstruction result the voxels will depict these gaps that do not represent the true anatomy. Intensity interpolation techniques have been used to fill in these gaps, which introduces false information degrading the resolution of the reconstructed image. One of the great advantages of this reconstruction approach is that the original information is not modified, which allows the image to be repeatedly processed. It is possible to apply various rendering techniques, segmentation and classification, and volume measurement.

3.5 Effects of errors in reconstruction

Except for systems using 2D arrays, 3D ultrasound images are reconstructed from multiple 2D images, knowing their relative position and orientation. In this sense, geometric distortions in the reconstruction can be generated due to errors in the spatial location of the 2D images. Such distortions can generate errors in the measurement of lengths, areas and volumes of the anatomical structures contained in these images[43]. A large number of problems must be solved when combining 2D images on a 3D dataset. These problems can be divided into two categories: non-uniformity of intensities and spatial non-uniformity.

3.5.1 Non-uniformity of intensities

The average and distribution of intensities for a 2D image depend on both the ultrasound imaging system and the material properties. The image intensities also depend on the geometry, size, pulse frequency, pulse amplitude and the type of beam focusing shape by the transducer. Effects such as shading and enhancement also affect the average image intensities. Among the parameters that must be controlled in an ultrasound system are: 1) overall gain, 2) dynamic range of deployment, 3) focusing parameters, 4) scan line density, 5) pulse amplitude, 6) scan angular range, and 8) spatial rescaling of the image.

All these features of ultrasound technology cause variation in the values assigned to the intensities between 2D images. These effects are difficult

to model and therefore to remove. The fundamental idea then to reduce these effects is to perform a correct tuning of the ultrasound acquisition parameters[30]. Another approach that has been proposed in the literature is to visualize the acquisition error compensation process as an optimization procedure, based on the fact that data inconsistency generates discontinuities in the reconstructed object. Considering a deformable surface model, which represents the object to be reconstructed, it is reasonable to think that the acquisition errors can be compensated by minimizing the energy functional associated with the 2D model, with respect to the position of the scanned planes[37].

3.5.2 Spatial non-uniformity

The voxel dimensions are reflected in the spatial resolution of the images. However, the axial, lateral and sampling resolution of 3D ultrasound are all different. A voxel of smaller size at the lower resolution would minimize the loss of image detail. In many scanning systems, larger voxel sizes are used to reduce the amount of storage memory and rendering times. Voxel filling techniques may be required in regions of the volume with low sampling resolution. Alternatives can be used to fill the gaps between images, such as neighboring element interpolation[29], or convolution of the 2D images with a Gaussian filter[10]. In general, interpolation of the data is necessary to obtain a regular voxel array such that the reconstructed objects can be displayed and/or compared with other imaging modalities[29].

4. Three-dimensional visualization

There is a wide variety of computational methods for 3D visualization of medical images in research and clinical applications[44-46]. The effectiveness of the technique depends essentially on the image generating source and the fidelity of the three-dimensional reconstruction. Probably the most important factor in the development of volume visualization techniques is that the data has a dimension beyond the display capacity of the computer, hence the visualization technique used often plays a very important role in determining the information that is transmitted to the operator. In 3D ultrasound, three different visualization techniques have been used: surface rendering, multiplanar recomposition and volumetric rendering.

4.1 Surface rendering

Several semi-automatic[39,42,26] and automatic methods[11,35,36,41] have been proposed for the identification of cardiovascular structures. For the restoration processes of cardiovascular surfaces in 3D ultrasound, spatial filtering techniques[12], computer vision and neural network techniques[37], mesh set generation[47] and deformable surfaces[26,48] have been used.

4.2 Multiplanar recomposition

In 3D ultrasound, the use of two multiplanar recomposition techniques has been reported: orthogonal planes and cube view.

4.2.1 Orthogonal planes

This visualization tool allows the simultaneous display of the intersection of three orthogonal planes. Additionally, the tool allows to control the intersection point, the viewing angle, the number of 2D planes, and the scale. **Figure 6** shows an example of this type of visualization technique.

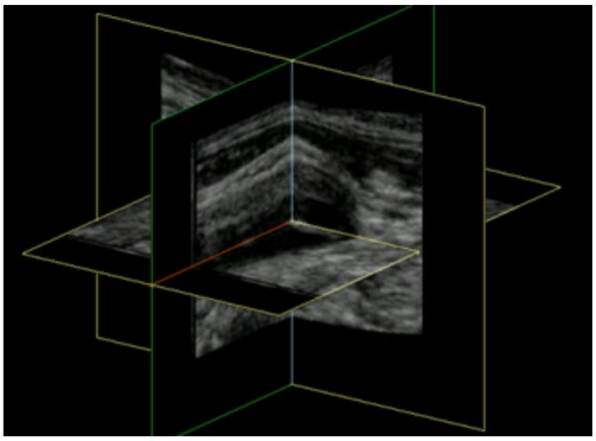

Figure 6. Multiplanar recomposition by orthogonal planes.

4.2.2 Cube view

The image is presented as a polyhedron, which represents the boundaries of the reconstructed volume (**Figure 7**). Each of the multiple faces of the polyhedron is determined by rendering the appropriate 2D image using texture mapping techniques. Visualization tools allow selecting any face and moving it into or out of the volume.

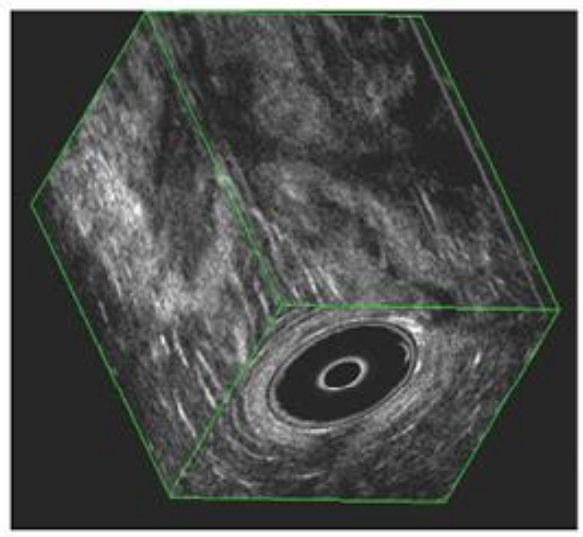

Figure 7. Multiplanar recomposition cube view.

4.3 Volumetric rendering

Volumetric rendering has been used to visualize the result of applying 3D segmentation of the left ventricle[35,49] and 3D filtering of images of the heart chamber[50]. Approaches based on maximum intensity projections in which only the voxel of maximum intensity along each beam is displayed have been used to visualize intravascular ultrasound images[51].

5. Advances in three-dimensional echocardiography

The advances achieved in three-dimensional cardiac ultrasound imaging in recent years cover different areas such as 3D acquisition systems[52,53], preprocessing techniques[26,47,50], quantification[49,54], and fusion with other imaging modalities[51].

5.1 Acquisition systems

The trends for the improvement of 3D ultrasound image acquisition systems are leaning towards the development of new transducer array technologies, which make it possible to reduce the high cost in the implementation of such designs, gaining high 3D acquisition speeds with a high degree of accuracy[52]. On the other hand, the design of robot-assisted systems for medical ultrasound diagnosis is also part of the new trends in the implementation of 3D acquisition systems[53].

5.1.1 New transducer array technologies

Hossack *et al.*[52] have proposed a diagnostic ultrasound system using modified transducer arrays, in which 3D ultrasound data are accurately acquired from multiple 2D images. The system is based on the use of a linear phased array, whose structure comprises a central one-dimensional (1D) linear array, which is responsible for acquiring the image. On both sides of the 1D array, oriented perpendicularly, motion tracking arrays are placed. All arrays acquire images by B-scan. The images acquired by the tracking arrays are essentially coplanar, and therefore suitable for matching features between consecutively acquired 2D images. This capability is used for motion identification, by searching for some kind of correlation between sequentially acquired images. A minimum sum of the absolute differences algorithm (MSDA) of the images obtained by the tracking arrays is used to obtain an estimate of the motion. The three arrays are designed such that the center frequency is the same and their elements are equally spaced.

The ultrasound beamforming is programmatically controlled, allowing the three transducer arrays to operate as a single transducer. If the definition of the beam aperture size is carefully controlled, no crossover of the transmit and/or receive channels of each of the three arrays will ever occur. The system has been used for fast 3D color Doppler ultrasound acquisition in the estimation of carotid artery stenosis, allowing surface rendering visualization of these structures. The average acquisition time was 12 minutes, compared to the 45 minutes required by a conventional duplex sonographer. This new method was subjected to a small clinical validation, the results of which indicate that the system can be clinically used in the acquisition of 3D ultrasound data quickly and with a high degree of accuracy.

5.1.2 Robot-assisted ultrasound systems

A robot-assisted ultrasound diagnostic system has been developed by Abolmaesumi *et al.*[53] to acquire and display 3D ultrasound images in real time, incorporating the ability to automatically track a feature located within the 3D image. The system consists of a manual master controller, a slave manipulator on which the ultrasound transducer is mounted, and a computer-controlled system that

allows the operator to remotely position the ultrasound transducer with respect to the patient's body. This robot has initially been used to examine the carotid arteries in the diagnosis of occlusions in the branches of these arteries. The system uses a shared controller that is capable of simultaneously acquiring images, and controlling the mobility and strength of the mechanical arm. The ability to automatically guide the ultrasound transducer as a function of the images it acquires is a useful feature in diagnostic scans when used in conjunction with supervised control to reduce operator fatigue.

During the scan, the operator with the graphical user interface and handheld controller generates a series of commands which are coordinated by a visual servo-system, which is charged with controlling the robot and thus the movement of the ultrasound transducer. The ultrasound images are acquired in real time and displayed on the user interface, using surface rendering, together with a 3D model by volumetric rendering of the transducer. Features from the ultrasound image are selected with the help of the mouse, which are used as inputs to the feature tracking controller, which is responsible for guiding the robot's movements. Five types of feature tracking models are presented: cross-correlation algorithm, spatial similarity detection, the Star algorithm, Star-Kalman algorithm and a discrete active model. These methods have been compared in carotid artery tracking, with the similarity detection method and the Star-Kalman algorithm demonstrating excellent ability to track features with motions greater than 200 pixels/s, however, the Star-Kalman algorithm requires less computational time.

The cross-correlation and Star algorithms were not able to track the features in the arteries. The discrete active model was not able to track features with movements greater than 100 pixels/s. The system has proven to be applicable in 3D reconstruction and teleultrasound. Other potential applications are image-guided interventions, exploration and registration with images obtained with other imaging modalities.

5.2 Preprocessing techniques

Filtering techniques and segmentation algorithms constitute the main areas of research and development on preprocessing techniques explored in recent years in three-dimensional ultrasound imaging.

5.2.1 Image filtering and enhancement

Tang *et al.*[50] propose a multidimensional image enhancement algorithm based on a fuzzy domain enhancement method, as well as on the implementation of recursive and separable low-pass filters. Transformations in the fuzzy domain have been employed to represent or manipulate data that are not distinct, but highly fuzzy. Fuzzy logic is employed as a simple transformation of both the dynamic range and local variations of gray levels over the fuzzy domain by generating a fuzzy image using image smoothing techniques. Generally, smoothed images are obtained by the application of kernel-based methods, such as averaging operators or Gaussian operators; but the computational complexity, especially in 3D images, increases considerably when the kernel size is increased (kernel size must be smaller than 5 × 5 pixels). Two low-pass filters are introduced, one based on separable Butterworth low-pass filters and the other based on the Deriche-Monga principle, which satisfies the Canny design criterion.

The fuzzy image thus obtained is transformed to the fuzzy domain using different membership functions, which are responsible for transforming the dynamic range of the image, transforming the image details, and transforming the details of a noisy image. After transforming the dynamic range and image components to the diffuse domain, it is possible to define an enhancement function, which depends on the degree of fusification of the transformed image and has the ability to adjust the dynamic range of the image and to enhance or filter the image details. By applying an inverse transform of the fuzzy domain, it is possible to obtain the resulting enhanced image. Enhancement is often used in conjunction with other image processing algorithms, such as segmentation, feature extraction and visualization. 3D image filtering and enhancement is an important step in improving three-dimensional visualization. Enhancing images while reducing the influence of background and noise levels improves

the visualization of structural information using volumetric rendering techniques.

The enhancement algorithm has been tested on ultrasound images of the cardiac cavities, being computationally efficient and showing a smooth and natural enhancement. Real-time implementation is possible because the smoothing procedure is separable in each dimension and can be performed recursively with low computational cost.

5.2.2 Segmentation algorithms in intravascular ultrasound

Intravascular ultrasound (IVUS) provides a direct anatomical description of the coronary arteries, including plaques and areas, which is important in quantitative studies of coronary artery damage. Traditionally these studies are performed manually, which is a laborious, time-consuming procedure subject to inter- and intra-observer variability. Klingensmith *et al.*[26] have proposed a new technique called active surface segmentation, which eliminates many of the aforementioned problems by developing a semi-automated segmentation algorithm for edge identification in IVUS images. The active surface is an extension of 3D active contour models. Given an initial 3D model, it is subjected to deformations, which is controlled by energy minimization processes associated with such model. The initial model corresponds to a cylindrical surface, which is generated by linear interpolation of manually set contours in the first, last and some intermediate images, with a fixed number of vertices.

The active 3D model considers that the energy functional to be minimized should control both the continuity and the curvature of the final 3D model, and additionally, it should have the possibility of following a certain characteristic of the image, which in this case is defined by the transition in radial direction from a light to a dark region, which corresponds to the transition of the arterial wall borders. The method has been subjected to clinical validation, achieving an accurate description of the coronary morphology.

5.2.3 Carotid artery segmentation algorithms

Gill *et al.*[47] have reported a semiautomated method for segmentation of 3D ultrasound images of the carotid arteries. The method is based on a dynamic balloon model represented by a triangular mesh. The mesh is manually placed inside the carotid arteries and then pushed towards the artery wall by applying an inflation force to the mesh vertices in a direction normal to the mesh surface. When equilibrium is reached between the inflation forces, the final model represents the proper shape of the artery. This final model is subsequently deformed by means of a force defined from the image data, which attracts the model to the 3D contours, with the property that the minimum of that force is reached when the mesh coincides with the artery wall.

The semi-automatic segmentation method is compared to a fully manual segmentation method, finding that the semi-automatic technique is more stable in terms of intra-observer variability than the manual method. Additionally, they examine the accuracy of their method by comparison with ideal surfaces, determined by the average of surfaces segmented manually by different specialists. It is shown that the method for freehand 3D ultrasound segmentation of carotid arteries produces meshes that effectively approximate the average of manually segmented surfaces, with local variability as a function of initial model position, but less variable than manual segmentation.

5.3 Quantification

Angelini *et al.*[49] have presented a four-dimensional (4D) spatiotemporal analysis method (3D + time) for real-time three-dimensional ultrasound filtering and enhancement, and for quantitative assessment of ventricular function by cardiac ultrasound. Speckle noise (phase effects) distorts ultrasound data by introducing abrupt changes in the intensity profiles in the image, while varying the attenuation of the intensities of identical cardiac structures. This makes the spatial imaging domain inhomogeneous, and suggests that measurements are based on phase information rather than intensity profiles. A new family of wavelets called brushlet functions, based on Fourier transform expansion, are used to obtain a redundant representation of the image.

This redundant multiscale representation is appropriate in image analysis and enhancement,

because it allows the image to be decomposed into different patterns in the form of oriented harmonics, which are invariant to intensity and contrast ranges. On the other hand, the transformation is a homomorphism between the location points of the data in the original set and the position of the coefficients in each projected feature or pattern. To extract the features of interest and eliminate speckle noise components, a thresholding process is applied to the coefficients in the transformed domain. Once the image is filtered and re-thresholded, a contour segmentation process is applied to the image by deformable models. A balloon model is implemented, using a finite difference scheme. The initial contour is defined by a circle with a radius equal to five pixels located inside the cavity to be segmented. The center of the circle was identified by a Hough transform applied to the contours extracted with a Prewitt filter for every ten 2D images of the volume.

After segmentation, the left ventricular cavity is reconstructed and end-diastolic and end-systolic volumes and ejection fraction are calculated. The system has been validated with a database of six clinical cases of magnetic resonance imaging, and with a set of contrast echocardiography images in phantoms. The authors conclude from the set of experiments performed that it is possible to extract the endocardial borders of the left ventricle using 2D deformable models and it is possible to quantify volumes of interest with a higher degree of accuracy than those found by manual techniques. The authors intend to extend the segmentation process to higher dimensions, thereby ensuring the continuity of ultrasound data in time and space.

5.4 Fusion with other imaging modalities

The objective of multimodal image registration and fusion (grouping of data types) is to combine types of information from complementary imaging modalities. Wahle *et al.*[51] combine geometric information obtained from biplane angiography with volumetric data derived from intravascular ultrasound for reconstruction of the coronary arteries. The catheter trajectory is extracted and reconstructed from biplane angiography and used to project the intravascular ultrasound at its locations. For the reconstruction process of the biplane images, it is necessary to have an accurate description of the image geometry. The reconstruction system adopted has been developed at the German Heart Institute in Berlin. An algorithm for extracting the catheter trajectory, based on dynamic programming, and allowing free manipulation of the regions of interest, is derived from Catmull-Rom splines. The 2D ultrasound images are segmented by an algorithm based on graph search in a given elliptical region of interest. The whole process is automatic, except for the definition of the region of interest. The location of the intravascular ultrasound frames and the relative orientations of one with respect to the other is calculated using a discrete approximation of the Frenet-Serret formula of differential geometry. The absolute orientation of the image set is established, using the catheter images as an artificial landmark. The fusion has been extensively validated in computational simulations, phantoms and pig hearts.

6. Conclusions

Three-dimensional cardiac ultrasound imaging constitutes a multidimensional imaging modality with great perspectives in clinical cardiac diagnosis. Various advances in acquisition, preprocessing, analysis and visualization place 3D ultrasound in a competitive position with respect to other imaging modalities. However, the treatment of this type of images is still an open problem, with several trends in the field of research. All these trends have to face two complex problems to be solved: computational cost vs. accuracy of the results obtained. And to all this we can add the difficult task of performing a fairly efficient clinical validation of the computational systems proposed or to be proposed.

Acknowledgments

This work was funded by the Research Department of the Universidad Nacional Experimental del Táchira, San Cristóbal, Venezuela.

Conflict of interest

The authors declare that they have no conflict of interest.

References

1. Nelson TR, Downey DB, Pretorius DH, *et al*. Three-dimensional ultrasound. Philadelphia: Lippincott Williams & Wilkins; 1999.
2. Kremkau FW. Diagnostic ultrasound: Principles and instruments. Philadelphia: W.B. Saunders Company; 1993.
3. Geiser EA, Oliver LH. Echocardiography physics and intrumentation. In: Collins S, Skorton D (editors). Cardiac imaging and image processing. New York: McGraw Hill; 1980. p. 24–38.
4. Crawford D, Bell D, Bamber J. Compensation for the signal processing characteristic of ultrasound b-mode scanners in adaptive speckle reduction. Ultrasound in Medicine & Biology 1993; 19(6): 469–485.
5. Nelson T, Pretorius D. 3D ultrasound image quality improvement using spatial compounding and 3D filtering. Medical Physics 1994; 21(6): 998–999.
6. Kotropoulos C, Magnisalis X, Pitas I, *et al*. Nonlinear ultrasonic image processing based on signal-adaptive filters and self-organizing neural networks. IEEE Transactionson Image Processing 1994; 3(1): 65–77.
7. Gronningsaeter A, Angelsen BAJ, Gresli A, *et al*. Blood noise reduction in intravascular ultrasound imaging. IEEE Transactions on Ultrasonics, Ferroelectrics, and Frequency Control 1995; 42(2): 200–209.
8. Fortes JMP. A closed loop ML algorithm for phase aberration correction in phased array imaging systems. I: Algorithm synthesis and experimental results [Ultrasound medical imaging]. IEEE Transactions on Ultrasonics, Ferroelectrics, and Frequency Control 1997; 44(2): 259–270.
9. Achim A, Bezerianos A, Tsakalides P. Novel bayesian multiscale method for speckle removal in medical ultrasound images. IEEE Transaction on Medical Imaging 2001; 20(8): 772–783.
10. Hajnal JV, Hill DLG, Hawkes DJ. Medical image registration. New York: CRC Press LLC; 2001.
11. Zhang X, McKay CR, Sonka M. Tissue characterization in intravascular ultrasound imaging. IEEE Transaction on Medical Imaging 1998; 17(6): 889–899.
12. Canals R, Lamarque G, Chatain P. Volumetric ultrasound system for left ventricle motion imaging. IEEE Transactions on Ultrasonics, Ferroelectrics, and Frequency Control 1999; 46(6): 1527–1538.
13. Light ED, Idriss SF, Wolf PD, *et al*. Real-time three-dimensional intracardiac echocardiography. Ultrasound in Medicine & Biology 2002; 27(9): 1177–1183.
14. Xiao G, Brady JM, Noble JA, *et al*. Nonrigid registration of 3D free-hand ultrasound images of the breast. IEEE Transaction on Medical Imaging 2002; 21(4): 405–412.
15. Deng J, Sullivan ID, Yates R, *et al*. Real-time three-dimensional fetal echocardiography—Optimal imaging windows. Ultrasound in Medicine & Biology 2002; 28(9): 1099–1105.
16. Volkmer BG, Nesslauer T, Kuefer R, *et al*. Visualization of urinary stones by 3D ultrasound with surface rendering. Ultrasound in Medicine & Biology 2002; 28(2): 143–147.
17. Pretorius DH, Nelson TR. Three-dimensional ultrasound. Ultrasound in Obstetrics and Gynecology 1995; 5: 219–221.
18. Fenster A, Downey DB. 3D ultrasound imaging: A review. IEEE Engineering in Medicine and Biology 1996; 15(6): 41–51.
19. Raab FH, Blood EB, Steiner TO, *et al*. Magnetic position and orientation tracking system. IEEE Transaction on Aerospace and Electronic Systems 1979; 15(15): 709–717.
20. Birkfellner W, Watzinger F, Wanschitz F, *et al*. Systematic distortions in magnetic position digitizers. Medical Physics 1998; 25(11): 2242–2248.
21. Moritz WE, Pearlman AS, McCabe DH, *et al*. An ultrasonic technique for imaging the ventricle in three dimensions and calculating its volume. IEEE Transaction on Biomedical Engineering 1983; 30(8): 482–492.
22. Sato Y, Nakamoto M, Tamaki Y, *et al*. Image guidance of breast cancer surgery using 3D ultra-sound images and augmented reality visualization. IEEE Transaction on Medical Imaging 1998; 17(5): 681–693.
23. Martin RW, Bashein G, Detmer PR, *et al*. Ventricular volume measurement from a multiplanar transplanar transesophageal ultrasonic imaging systems: An in vitro study. IEEE Transaction on Biomedical Engineering 1990; 37(5): 442–449.
24. Smith SW, Pavy HE, von Ramm OT. High speed ultrasound volumetric imaging system part I: Transducer design and beam steering. IEEE Transactions on Ultrasonics Ferroelectrics and Frequency Control 1991; 38(2): 100–108.
25. Light ED, Davidsen RE, Fiering JO, *et al*. Progress in two dimensional arrays for real time volumetric imaging. Ultrasonic Imaging 1998; 20(1): 1–18.
26. Klingensmith JD, Shekhar R, Vince DG. Evaluation of three-dimensional segmentation algorithms for the identification of luminal and medial-adventitial borders in intravascular ultrasound images. IEEE Transactions on Medical Imaging 2000; 19(10): 996–1011.
27. Woods R. Handbook of medical image processing and analysis. San Diego: Academic Press; 2000.
28. Prager RW, Rohling RN, Gee AH, *et al*. Rapid calibration for 3-D freehand ultrasound. Ultrasound in Medicine & Biology 1998; 24(6): 855–869.
29. Rohling R, Gee A, Berman L. A comparison of freehand three-dimensional ultrasound reconstruction techniques. Medical Image Analysis 1999; 3(4): 339–359.
30. Aiger D, Cohen-Or D. Mosaicing ultrasonic volumes for visual simulation. IEEE Computer Graphics and Applications 2000; 20(2): 53–61.
31. Krücker JF, Meyer CR, LeCarpentier GL, *et al*. 3D spatial compounding of ultrasound images using

image-based nonrigid registration. Ultrasound in Medicine & Biology 2000; 26(9): 1475–1488.
32. Tong S, Cardinal HN, McLoughlin RF, *et al*. Intra- and inter-observer variability and reliability of prostate volume measurement via two-dimensional and three-dimensional ultrasound imaging. Ultrasound in Medicine & Biology 1998; 24(5): 673–681.
33. Cardinal HN, Gill JD, Fenster A. Analysis of geometrical distortion and statistical variance in length, area, and volume in a linearly scanned 3-D ultrasound image. IEEE Transactions on Medical Imaging 2000; 19(6): 632–651.
34. Dias JMB, Leitao JMN. Wall position and thickness estimation from sequences of echocardiographic images. IEEE Transactions on Medical Imaging 1996; 15(1): 25–38.
35. Xiao G, Brady M, Noble JA, *et al*. Segmentation of ultrasound b-mode images with intensity inhomogeneity correction. IEEE Transactions on Medical Imaging 2002; 21(1): 48–57.
36. Setarehdan GK, Soraghan JJ. Automatic cardiac LV boundary detection and tracking using hybrid fuzzy temporal and fuzzy multiscale edge detection. IEEE Transactions on Biomedical Engineering 1999; 46(11): 1364–1378.
37. Coppini G, Poli R, Valli G. Recovery of the 3D shape of the left ventricle from echocardiographic images. IEEE Transactions on Biomedical Engineering 1996; 14(2): 301–317.
38. Detmer PR, Bashein G, Martin RW. Matched filter identification of left-ventricular endocardial borders in transesophageal echocardiograms. IEEE Transactions on Medical Imaging 1990; 9(4): 396–404.
39. Chalana V, Linker DT, Haynor DR, *et al*. A multiple active contour model for cardiac boundary detection on echocardiographic sequence. IEEE Transactions on Medical Imaging 1996; 15(6): 290–298.
40. Mikic I, Krucinski S, Thomas JD. Segmentation and tracking in echocardiographic sequences: Active contours guided by optical flow estimates. IEEE Transactions on Medical Imaging 1998; 17(2): 274–284.
41. Malassiotis S, Strintzis MG. Tracking the left ventricle in echocardio-graphic images by learning heart dynamics. IEEE Transactions on Medical Imaging 1999; 18(3): 282–290.
42. Jacob G, Noble JA, Behrenbruch C, *et al*. A shape-space-based approach to tracking myocardial borders and quantifying regional left-ventricular function applied in echocardiography. IEEE Transactions on Medical Imaging 2000; 21(3): 226–238.
43. Goldstein A. Errors in ultrasound digital image distance measurements. Ultrasound in Medicine & Biology 2000; 26(7): 1125–1132.
44. Stytz MR, Frieder G, Frieder O. Three-dimensional medical imaging: Algorithms and computer systems. ACM Computing Surveys 1991; 23(4): 421–499.
45. Nelson TR, Elvins TT. Visualization of 3D ultrasound data. IEEE Computer Graphics and Applications 1993; 13(6): 50–57.
46. Hauser H, Mroz L, Bischi GI, *et al*. Two-level volume rendering. IEEE Transactions on Visualization and Computer Graphics 2001; 7(3): 242–252.
47. Gill JD, Ladak HM, Steinman DA, *et al*. Accuracy and variability assessment of a semiautomatic technique for segmentation of the carotid arteries from three-dimensional ultrasound images. Medical Physics 2000; 27(6): 1333–1342.
48. Bardinet E, Cohen L, Ayache N. Tracking and motion analysis of the left ventricle with deformable superquadrics. Medical Image Analysis 1996; 1(2): 129–149.
49. Angelini ED, Laine AF, Takuma S, *et al*. LV volume quantification via spatiotemporal analysis of real-time 3D echocardiography. IEEE Transactions on Medical Imaging 2001; 20(2): 457–469.
50. Tang H, Zhuang T, Wu E. Realizations of fast 2D/3D image filtering and enhancement. IEEE Transactions on Medical Imaging 2001; 20(2): 132–140.
51. Wahle A, Prause GPM, DeJong SC, *et al*. Geometrically correct 3D reconstruction of intravascular ultrasound images by fusion with biplane angiography: Methods and validation. IEEE Transactions on Medical Imaging 1999; 18(8): 686–699.
52. Hossack JA, Sumanaweera TS, Napel S, *et al*. Quantitative 3D diagnostic ultrasound imaging using a modified transducer array and an automated image tracking technique. IEEE Transactions on Ultrasonics Ferroelectrics and Frequency Control 2002; 38(2): 1029–1038.
53. Abolmaesumi P, Salcudean SE, Zhu W, *et al*. Image-guided control of a robot for medical ultrasound. IEEE Transaction on Robotics and Automation 2002; 18(1): 11–23.
54. G ́erard O, Billon AC, Rouet JM, *et al*. Efficient model-based quantification of left ventricular function in 3D echocardiography. IEEE Transactions on Medical Imaging 2002; 21(7): 1059–1068.